Total-energy local-density studies of the α-γ phase transition in Ce

B. I. Min, H. J. F. Jansen,* and T. Oguchi

Department of Physics and Astronomy, Northwestern University, Evanston, Illinois 60201

A. J. Freeman

Department of Physics and Astronomy, Northwestern University, Evanston, Illinois 60201
and Los Alamos National Laboratory, University of California, Los Alamos, New Mexico 87545

(Received 16 December 1985)

The ground-state properties of Ce metal are investigated using total-energy full-potential linearized augmented plane wave and linearized muffin-tin orbital band-structure methods within the local spin-density functional approximation. The energetics involved in the α-γ phase transition are determined and discussed. For both paramagnetic and ferromagnetic cases, the electronic structures, density of states, charge densities, and total energies are presented as a function of the lattice parameter in order to assess the nature of the transformation with pressure, associated with a Mott-type transition in the $4f$ electrons. Stoner factor and electron-phonon coupling parameters are evaluated in order to discuss the magnetic and superconducting properties of Ce metal under pressure.

I. INTRODUCTION

Ce metal has unique properties compared with neighboring elements in the rare-earth series. It is generally believed that f electrons in most of the rare-earth metals are located far inside the s and d conduction-band orbitals to behave as localized core electrons. However, f electrons in Ce are much more extended and thus f-d hybridization and even f-f direct interactions between nearest neighbors are not small. As a result, Ce shows intermediate behavior and exhibits both localized and delocalized (itinerant) properties which leads to many intriguing manifestations expected of Fermi-liquid, mixed-valence, and Kondo systems, etc. Thus, Ce shows either a magnetic or a superconducting phase depending upon temperature and pressure.[1] fcc α-Ce, which is the most stable phase at normal pressure, behaves as an enhanced Pauli paramagnetic metal, and becomes a superconductor below 50 mK at a pressure of 40 kbar. With increasing temperature, α-Ce transforms at ambient pressure to double hcp β-Ce at $T=95$ K and to fcc γ-Ce at $T=263$ K. Both of these phases show magnetic behavior in that their susceptibilities follow a Curie-Weiss law, which is taken to indicate that the f electrons in β-Ce and γ-Ce are localized to form magnetic moments. At higher pressure, α-Ce transforms to orthorhombic α'-Ce which is a superconductor with $T_c = 1.9$ K.

The most fascinating property of Ce metal is the occurrence of the γ-α isostructural (fcc-to-fcc) transition, which ends in a critical point[2] near 550 K and 18 kbar in analogy to the well-known liquid-gas phase transition. A large volume (a 17% decrease) and loss of magnetic moment follow in going from γ- to α-Ce. The γ-α transition was originally suggested[3] to be a valence transition in which a magnetic localized $4f$ electron is partially promoted into the conduction band to form an intermediate valence[4] phase in α-Ce (promotional model). Various recent experiments, however, indicate that there is no appreciable change in the number of $4f$ electrons at the γ-α transition, whereas the promotional model requires a change of about 50%. On the other hand, Gustafson et al.[5] proposed delocalization of the $4f$ electrons into a band state. Johansson[6] extended this idea to point out, on the basis of empirical data, the possibility of a Mott-like transition in which the γ phase is the low density insulator side of a Mott transition and that under pressure a localization-delocalization transition of the $4f$ electron occurs with a concomitant loss of magnetic moment. These arguments appear to be consistent with most of the experimental measurements and, in fact, several band-structure calculations[7-9] show that the $4f$ band in α-Ce is over 1 eV wide and that the number of f electrons changes only slightly from γ to α in support of Johansson's Mott transition model.

Recent valence-band photoemission (PE) experiments,[10] which exhibit a double-peak structure associated with the $4f$ electrons, with a peak near E_F and another about 2 eV below E_F, have given rise to interesting controversies about their origin. There appears to be only a small difference (in shape and peak position) between the spectra of γ-Ce and α-Ce. In contrast, the total density of states from band-structure calculations shows only one peak of f character near E_F and another of s-d character 1.3 eV below E_F for both materials.

Many theoretical models were proposed to interpret this anomalous two-peak structure in relation to the γ-α transition. Allen and Martin[11] and Lavagna et al.[12] used the concept of a Kondo lattice model[13] to successfully account for the thermodynamics of the γ-α transition and interpreted the peak near E_F as a Kondo resonance peak. Gunnarsson and Schönhammer[14] reproduced the two-peak structure of Ce with the Anderson model by considering available final states. Fujimori[15] also discussed the PE spectra with the similar concept of hybridization using

a cluster approach. Hüfner and Steiner[16] considered the different channels for the screening of the 4f excitations to suggest the final-state effects of PE. Liu and Ho[17] took into account the final-state concept in emphasizing the large Coulomb correlation interaction between 4f hole and the conduction electrons. All of these models assume the constancy of the number of the f electrons during the γ-α transition.

Since high-energy experiments such as PE observe excited-state properties, an energy-band calculation which is essentially a ground-state description may not be appropriate to analyze experiment. The validity of the band description for the strongly correlated f-band materials is still questionable. The eigenvalues in the local-density approximation (LDA),[18] which are obtained in band-structure calculations, lack physical meaning especially for very localized narrow-band electrons. Thus, total energy calculations for the initial and final state are necessary to determine the energy of the excitation. We discuss these excited-state properties elsewhere[19] using the total-energy band-structure method and thus in this paper we restrict ourselves to the ground-state properties of Ce metal.

An LDA band-structure calculation is expected to yield a good description of the ground-state properties of rather extended 4f-band Ce metal, provided it is carried out to self-consistency. Kmetko and Hill[20] performed the first self-consistent augmented-plane-wave (APW) band-structure calculation for γ- and α'-Ce and pointed out the increase in hybridization of the 4f states with the conduction band with reduction of the atomic volume. Glötzel[7] reported the cohesive and magnetic properties of fcc Ce obtained with the self-consistent relativistic linear muffin-tin orbital (LMTO) method[21] and found spin polarization to occur near the lattice constant of γ-Ce, which is related to the localization of the f electrons. Pickett et al.[8] performed self-consistent relativistic linearized APW band-structure[21,22] calculations for both the α and γ phases of Ce metal which included the nonspherical potential as well as spin-orbit coupling by perturbation theory and discussed the electronic and magnetic properties of Ce metal. Podloucky and Glötzel[9] studied the ground-state cohesive properties and calculated Compton profiles of γ- and α-Ce using the LMTO method to confirm the evidence against the promotional model.

It has been reported[23] that α-Ce undergoes a phase transition at 40 kbar and room temperature and that the superconducting T_c jumps by a factor of 40 up to 1.9 K. With greater pressure, T_c decreases. The high-pressure phase α'-Ce has an orthorhombic α-U structure, which is ascribed to the existence of itinerant f-bonding effects. Wittig[24] speculated from this that α'-Ce is a 4f-band metal, in which delocalized f-band electrons hybridized with the conduction band are responsible for the high T_c of α'-Ce. However, the effects of f electrons on the superconducting properties still appear to be in dispute.

In this paper, we report total-energy band-structure calculations undertaken to investigate the ground state properties of Ce by employing both the full-potential linearized APW (FLAPW) (Ref. 25) and the LMTO band-structure methods within the local-spin-density functional

approximation. The total energies of the paramagnetic and spin-polarized phases of Ce are used to discuss the energetics involved in the γ-α transition. In Sec. II, we describe briefly the methods used. In Secs. III and IV, the results of paramagnetic and spin-polarized band calculations are presented. The superconducting properties are discussed in Sec. V. The f-electron localization in the γ-α transition is discussed in Sec. VI and a discussion follows in Sec. VII.

II. DETAILS OF THE CALCULATION

The energy band structure of paramagnetic Ce metal was calculated self-consistently for a wide range of lattice constants using the full-potential linearized augmented-plane-wave (FLAPW) method within the local-density approximation. The core electrons were treated fully relativistically in the atomic central field approximation, while the valence electrons were obtained from the semi-relativistic[26] equations neglecting spin-orbit coupling. The periodic potential and charge density in the interstitial were expanded with 537 plane waves and in up to $l = 8$ Kubic harmonics inside the muffin-tin spheres. The eigenvalues were calculated at 80 k points in the $\frac{1}{48}$th irreducible part of the Brillouin zone in each iteration and for the exchange-correlation potential we use the prescription of von Barth and Hedin[27] with the parameters of Hedin and Lundqvist[28] and random-phase-approximation (RPA) scaling. For the Coulomb potential, the pseudo-charge method was adopted and the total energy was calculated with converged charge density and potential following the formulation of the local-density functional approximation.

The main features of the resulting band structures, densities of states, and Fermi surface are very close to those obtained previously by Pickett et al.[8] The one difference in our calculation from that of Pickett et al. is the way the 5p core electrons are treated. We find that the 5p electrons, which are located approximately 1 Ry below the conduction band, have a nonnegligible density outside the muffin-tin sphere, especially at smaller volumes (that is, at higher pressures). The interstitial 5p contribution amounts to almost 0.3 electrons in the case of α-Ce ($r_{\text{WS}} = 3.54$ a.u.; r_{WS} is the Wigner-Seitz radius) and this has a strong effect on the total energy. Hence we treat the 5p electrons in the same way as the valence electrons; we find a resulting bandwidth of almost 200 mRy for α-Ce. The effect of neglecting spin-orbit coupling of the 5p band is small on the total energy because this band is completely filled and the 5p-band contribution to the binding energy is much more important.

We use the LMTO band method for the description of the magnetic properties of Ce. In the LMTO band method, the Hamiltonian and overlap integrals of the muffin-tin orbitals are evaluated over the atomic Wigner-Seitz spheres, which are supposed to fill the unit-cell space. Thus, interstitial part of the unit cell is neglected. We consider the muffin-tin orbital basis functions up to $l = 3$ in the band-structure calculation and extend those up to $l = 4$ for an investigation of the superconductivity. The LMTO method is known to be suitable for close-packed

TABLE I. Calculated FLAPW partial density of states at E_F inside the muffin-tin sphere $N_l(E_F)$, in the interstitial $N^{int}(E_F)$, and total density of states $N^{tot}(E_F)$ (in states/Ry atom). Partial charges inside the muffin-tin sphere Q_l in the interstitial Q_{int}, the 4f-band width $W(4f)$ and the total energy E^{tot} as a function of Wigner-Seitz atomic radius r_{ws} (a.u.).

r_{ws}	$N_s(E_F)$	$N_p(E_F)$	$N_d(E_F)$	$N_f(E_F)$	$N_g(E_F)$	$N^{int}(E_F)$	$N^{tot}(E_F)$	Q_s	Q_p	Q_d	Q_f	Q_g	Q_{int}	$W(4f)$ (eV)	E^{tot} (Ry)
3.13	0.23	0.15	1.66	7.02	0.04	0.79	9.90	0.17	5.62	1.73	1.36	0.03	1.10	2.27	-17717.1852
3.27	0.99	0.29	2.61	11.96	0.07	1.76	17.68	0.21	5.72	1.73	1.28	0.02	1.03	2.00	-17717.1953
3.40	0.74	0.33	3.47	14.25	0.07	1.95	20.80	0.27	5.81	1.71	1.22	0.02	0.98	1.56	-17717.1957
3.54	1.48	0.62	6.37	25.27	0.10	3.75	37.58	0.31	5.86	1.65	1.19	0.02	0.98	1.23	-17717.1879
3.68	1.32	0.74	7.31	32.06	0.07	5.97	47.46	0.30	5.86	1.47	1.14	0.01	1.22	0.95	-17717.1782
3.81	1.52	0.82	8.82	41.13	0.10	4.62	57.00	0.41	5.96	1.60	1.18	0.01	0.84	0.78	-17717.1543

structures such as fcc Ce and in fact we find that the results obtained with the LMTO method are very close to those of the FLAPW as is discussed in the next section.

III. PARAMAGNETIC CALCULATIONS

The total-energy and band-structure results using the FLAPW method are given in Fig. 1 and Table I, respectively. The angular momentum decomposed densities of states and occupied charges inside the muffin tin and interstitial are provided in Table I as a function of Wigner-Seitz radius; the 4f bandwidths are also given for comparison. As is seen in Fig. 1, there is no evidence of any first-order structural transition in the total-energy curve and hence the γ-α phase transition apparently has a different origin. We notice, however, that with increasing pressure the number of 4f electrons increases and the 4f band broadens. The number of 4f electrons increases because the relative positions of s and p bands move up and these electrons are converted to d or f bands. The change in the number of 4f electrons, however, is only very small in going from γ-Ce to α-Ce. The band-broadening effect is clearly seen in the 4f bandwidth $W(4f)$, which is chosen as an eigenvalue difference of Γ'_2 and Γ_{25} at $k=0$. The values of $W(4f)$ are 0.78 eV for γ-Ce ($r_{ws}=3.81$ a.u.) and 1.23 eV for α-Ce ($r_{ws}=3.54$ a.u.). Due to this band broadening, the total density of states at the Fermi level $N(E_F)$ decreases from 57.0 states/Ry for γ-Ce to 37.6 states/Ry for α-Ce. The Fermi level is located near the bottom of a large f peak in all cases.

Our resulting cohesive energy (4.9 eV) is close to the experimental value (4.32 eV). The difference is attributed to errors made in the LDA treatment of the atom. For the energy of the atom, we use $-17\,716.8397$ Ry, which pertains to the LDA atomic ground-state configuration of $4f^{1.6}5d^{0.4}6s^2$. The equilibrium value of the Wigner-Seitz radius, $r^0_{ws}=3.35$ a.u., however, is almost 5% smaller
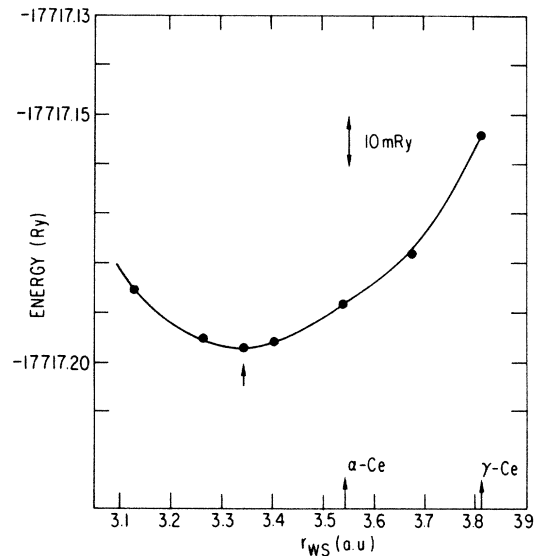

FIG. 1. FLAPW total-energy results as a function of Wigner-Seitz radius.

than the experimental value of α-Ce and the bulk modulus ($B = 0.56$ Mbar) is larger by a factor of 3. The reduction in the equilibrium lattice constant is related to the overestimated contribution of the $4f$-bonding effect in the local-density approximation which is common in the LDA description of localized bands. For example, our calculations[29] on Eu and Yb metals, in which the $4f$ electrons are very localized, show that their r_{WS}^0's are almost 12% and 7% smaller, respectively, and that the B's are almost 50% larger than the experimental values if we treat the $4f$ electrons as ordinary valence bands. In contrast to Eu and Yb, the $4f$ electrons in Ce are considered to be closer to the delocalized limit; nevertheless, even here the LDA description is not adequate in reproducing the correct behavior of the lattice constant.

In order to investigate this effect in more detail, we consider the following three cases for Ce by employing the LMTO method: (i) The $4f$ electrons are treated as ordinary valence band electrons; (ii) we treat one occupied $4f$ electron as belonging to the core, but still include the f-like radial functions in the description of the valence band; and (iii) we treat the one $4f$ electron as core and suppress f hybridization in the valence band completely.

We find that the overall results of the LMTO band-structure calculations are the same as those obtained with the FLAPW method; the shapes of their total energy curves are very similar, aside from a 0.3-eV upward shift in the absolute energy for the LMTO case. The equilibrium Wigner-Seitz radius obtained with the LMTO is 3.37 a.u. compared with 3.35 a.u. in FLAPW and the bulk modulus is 0.57 Mbar (LMTO) compared with 0.56 Mbar (FLAPW).

The resulting total-energy results for the three cases are displayed in Fig. 2 with the corresponding values of r_{WS}^0
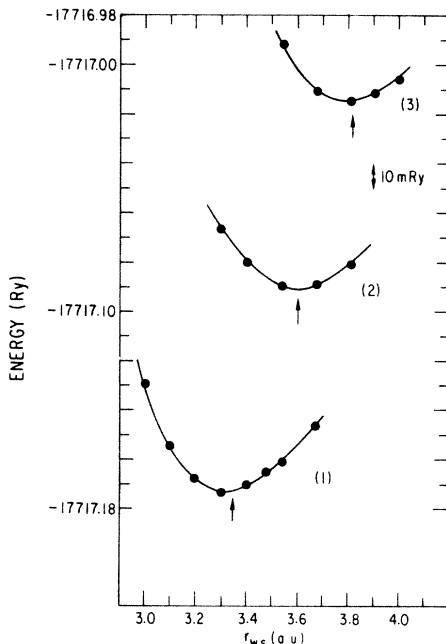
TABLE II. Calculated LMTO equilibrium Wigner-Seitz atomic radius r_{WS}^0, bulk modulus B, and total energy E_{tot}, for the three cases discussed in the text.

Case	r_{WS}^0 (a.u.)	B (Mbar)	E_{tot} (Ry)
1	3.34	0.69	$-17\,717.172$
2	3.61	0.52	$-17\,717.090$
3	3.82	0.56	$-17\,717.015$

and B, provided in Table II. In case (ii), we still find 0.4–0.7 f valence electrons in addition to the one $4f$ core electron consistent with the result of case (i) in which we obtain $1.4 \sim 1.7$ f valence electrons. The total density of states in cases (ii) and (iii) are greatly reduced due to the loss of one f valence electron. The equilibrium Wigner-Seitz radii are 3.35, 3.60, and 3.80 a.u., respectively, for the three cases. It is interesting to note that r_{WS}^0 of case (iii) is close to that of experiment for γ-Ce and that r_{WS}^0 of case (ii) is close to that of experiment for α-Ce (and is attributed to the bonding contribution of the f electrons). By treating the $4f$ electrons as core in case (ii) and (iii), we possibly mimic the localized properties of the f electrons; i.e., we neglect the hybridization between f and conduction electrons as well as the direct f-f hopping interaction between nearest neighbors. In fact, in a separate study,[29] we found that we well reproduce (within errors of less than 2%) the experimental lattice constants of the heavy rare-earth metals, if the f electrons are considered to be completely localized. Hence the agreement of the calculated equilibrium lattice constant in case (iii) and experiment for γ-Ce implies that the f electrons in γ-Ce do not contribute much to the cohesive properties, that is, they are in the localized limit. In comparison, the experimental equilibrium lattice constant of α-Ce is located between the results of case (i) and case (ii) [but closer to that of case (ii)], which apparently originates from the existence of partial bonding effects due to f electrons in α-Ce; f electrons are more or less delocalized at this atomic volume. These results suggest that two competing effects (f bonding and f localization) determine the stable phase under given external conditions so as to give rise to the γ-α transition. The localized nature of the f electrons can be also simulated by the inclusion of spin polarization—as will be discussed in the next section.

IV. SPIN-POLARIZED CALCULATIONS

We have performed local-spin-density calculations with the LMTO method in order to investigate the magnetic behavior of Ce metal at large volumes. From the self-consistent paramagnetic charge density, we first obtain the intra-atomic exchange correlation integral presented in Table III. The total density of states at E_F and angular momentum decomposed occupied charges are also given for comparison with the FLAPW results. The value of I_{xc} is almost constant, 0.42 eV (30 mRy), over the whole range of lattice constant, which indicates that I_{xc} is essentially a pressure-independent parameter. From the product $N(E_F)I_{xc}$, we can derive the Stoner enhancement factor $S = [1 - N(E_F)I_{xc}/2]^{-1}$; the calculations predict the

FIG. 2. LMTO total-energy results for the three cases, (1) itinerant, (2) partially localized (see text), and (3) localized f electrons.

TABLE III. Calculated LMTO charges (by l values) Q_l, the total density of states at E_F, $N(E_F)$ (in states/Ry atom), intra-atomic exchange correlation integral I_{xc}, Stoner enhancement factor S, and the total energy E_{tot}—all versus Wigner-Seitz radius r_{WS}.

r_{WS} (a.u.)	Q_s	Q_p	Q_d	Q_f	$N(E_F)$	I_{xc} (Ry)	$N(E_F)I_{xc}/2$	S	E_{tot} (Ry)
3.1	0.29	5.76	2.30	1.65	29.55	0.032	0.47	1.9	−17 717.1542
3.2	0.34	5.82	2.27	1.57	31.44	0.031	0.49	2.0	−17 717.1671
3.3	0.39	5.86	2.24	1.51	37.18	0.030	0.56	2.3	−17 717.1727
3.4	0.44	5.90	2.20	1.46	39.25	0.031	0.60	2.5	−17 717.1685
3.54	0.50	5.94	2.14	1.42	53.19	0.031	0.82	5.6	−17 717.1609
3.68	0.55	5.97	2.08	1.40	59.64	0.031	0.91	11.1	−17 717.1462
3.74	0.57	5.98	2.05	1.40	65.67	0.030	0.99	100.0	−17 717.1367
3.81	0.59	5.99	2.03	1.39	66.24	0.030	1.01	−10.0	−17 717.1259

occurrence of a ferromagnetic instability for values of r_{WS} larger than 3.74 a.u. This means that γ-Ce ($r_{WS}=3.81$) is located just in the ferromagnetically ordered region, which is consistent with the result of Glötzel.[7] The Stoner enhancement factor of α-Ce is still large ($S=5.6$) and so it behaves as a strongly exchange-enhanced paramag-

netic metal. [Recall that this is a similar to the case of Pd ($S=6.8$).[30]]

The total energies and magnetic moments obtained in the spin-polarized calculations are given in Table IV and Fig. 3. In agreement with the estimate of the Stoner instability, the total-energy difference between paramagnetic and ferromagnetic structures plotted in Fig. 4 shows that magnetic instability does occur for $r_{WS}\simeq3.7$ a.u. The total-energy difference between the two states is, however, very small; about 1 mRy for γ-Ce ($r_{WS}=3.81$). As is clear from Fig. 3(b), the spin-only magnetic moments ($4f$ and total) increase as one expands the volume; $4f$ moments are fully polarized for the atomic radius larger than 4.5 a.u. Furthermore, the band splitting in the spin-polarized calculation also supplies a value of I_{xc} from the relation $\Delta E = E_\uparrow - E_\downarrow = mI_{xc}$, where m is the spin magnetic moment. With $m=0.9$ and $\Delta E=0.03$ Ry at $k=0$ in the case of γ-Ce, we obtain $I_{xc}=33$ mRy, which is consistent with the result of the paramagnetic Stoner calculation ($I_{xc}=30$ mRy).

We have performed total-energy calculations at selected values of the lattice constant assuming the first kind of antiferromagnetic ordering in the fcc structure. The difference in total energy obtained for the antiferromagnetic state from that for the paramagnetic and ferromagnetic states is shown in Fig. 4. The ferromagnetic phase is seen to be more stable than the antiferromagnetic phase. Note that the energy differences between the different magnetic phases are very small, especially near the observed lattice constant of γ-Ce. At this lattice constant, the antiferromagnetic phase is more stable than the
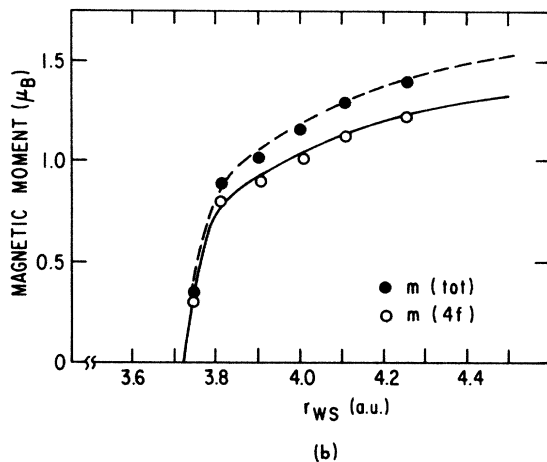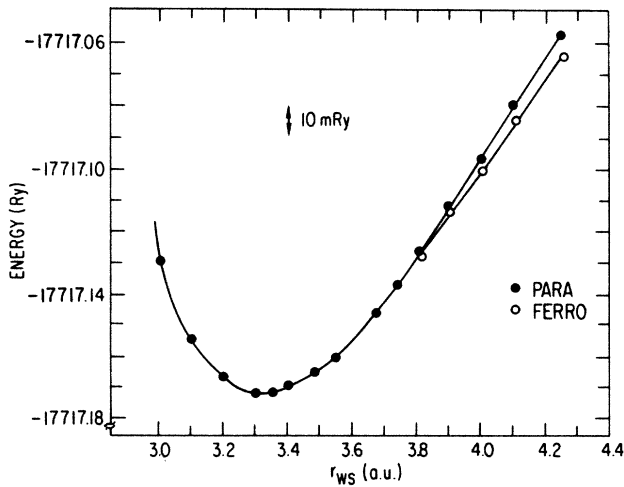

FIG. 3. (a) Paramagnetic and spin-polarized LMTO total-energy results as a function of Wigner-Seitz radius. (b) The $4f$ and total spin magnetic moments as a function of Wigner-Seitz radius.
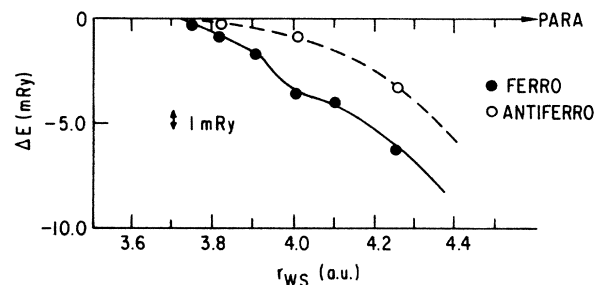

FIG. 4. LMTO total-energy differences between the ferromagnetic and antiferromagnetic phases with respect to that of paramagnetic phase as a function of Wigner-Seitz radius.

TABLE IV. Spin-polarized LMTO results for the total energy, the $4f$ and total spin magnetic moment (in Bohr magnetons), and the spin-up and spin-down density of states in E_F (in states/Ry spin)—all as functions of Wigner-Seitz radius r_{WS}.

r_{WS} (a.u.)	E_{tot} (Ry)	$m(4f)$ (μ_B)	m^{tot} (μ_B)	$N(E_F)$ ↑	$N(E_F)$ ↓
3.74	-17717.1369	0.31	0.34	40.4	24.4
3.81	-17717.1269	0.80	0.90	50.1	17.4
3.9	-17717.1132	0.90	1.02	69.3	14.7
4.0	-17717.1009	1.03	1.16	64.3	13.3
4.1	-17717.0835	1.13	1.30	88.9	12.6
4.25	-17717.0643	1.21	1.40	80.7	10.0

paramagnetic phase by 0.6 mRy ($=80$ K) but lies above the ferromagnetic phase by 0.4 mRy. These results are consistent with observations for the magnetic behavior of γ-Ce, which has a disordered magnetic structure at room temperature. Apparently then, no long-range magnetic order exists due to the competition of the three phases at room temperature; however, local moments are formed so that the susceptibility follows a Curie-Weiss law. These predictions for γ-Ce are consistent with the general view that γ-Ce is located in the low-density (localized f) side of Ce metal.

V. SUPERCONDUCTING PROPERTIES

We now consider the superconducting properties of Ce metal as a function of volume within the framework of the rigid muffin-tin approximation[31] (RMTA) and McMillan's[32] strong-coupling theory. The electron-phonon coupling constant λ is decomposed as

$$\lambda = \frac{N(E_F)}{2} \langle I^2 \rangle / M \langle \omega^2 \rangle = \eta / M \langle \omega^2 \rangle ,$$ (1)

where $N(E_F)$ is the total density of states, $\langle I^2 \rangle$ is the average electron-ion matrix element, M is the ionic mass, and $\langle \omega^2 \rangle$ is the average phonon frequency, squared. The electron stiffness parameter η in the RMTA is given by

$$\eta = \frac{4E_F}{\pi^2 N(E_F)} \sum_l (l+1)\sin^2(\delta_l - \delta_{l+1})$$
$$\times \frac{N_l(E_F)}{N_l^{(1)}(E_F)} \frac{N_{l+1}(E_F)}{N_{l+1}^{(1)}(E_F)} .$$ (2)

Here, $N_l(E_F)$ and $N_l^{(1)}(E_F)$ are the partial density of states of solid and single scatterer, respectively, and δ_l is the phase shift for the lth partial wave scattering from the spherical muffin-tin potential. We use the Allen-Dynes formula[33] to evaluate the transition temperature T_c;

$$T_c = \frac{\omega_{log}}{1.2} \exp\left[-\frac{1.04(1+\lambda)}{\lambda - \mu^*(1+0.62\lambda)} \right] .$$ (3)

Here, μ^* is the Coulomb pseudopotential parameter and $\omega_{log} = 0.87 \langle \omega^2 \rangle^{1/2}$.

We have investigated the superconducting properties of α- and γ-Ce using the self-consistent results obtained from our FLAPW calculations. The resulting values and parameters used in the calculation are given in Table V.

The results for the cases where the $5p$ electrons are treated (i) as band states or (ii) as core states are presented for comparison. When the $5p$ electrons are considered as valence and thus their hybridization is fully included, some p character at the Fermi level is lost. Hence the corresponding values of η (η_{sp} and η_{pd}) are reduced, as are λ and T_c, compared with the case where the $5p$ electrons are treated as core. As expected, the value of η increases in going from γ-Ce to α-Ce, whereas λ is larger for γ-Ce than for α-Ce due to the higher Debye temperature in α-Ce. Our estimated values of T_c in α-Ce are in reasonable agreement with experiment, $T_c < 0.01$ K. The superconducting transition temperature for γ-Ce has no physical meaning because the superconducting phase is suppressed by the magnetic phase, as discussed in the preceding section.

In order to examine the effect of pressure on the superconducting properties in more detail, we apply the RMTA for a wide range of Ce lattice constants using the self-consistent LMTO results. The muffin-tin potential in RMTA is replaced by an atomic sphere potential in this case and the $5p$ electrons are treated as valence band electrons. In the final self-consistent iteration with converged charge densities, the g states ($l=4$) are included in the basis set of muffin-tin orbitals. The results obtained using the LMTO atomic sphere potentials are very close to

TABLE V. Comparison of FLAPW calculated quantities (defined in the text) which appear in the calculation of the electron-phonon coupling parameter λ and the superconducting transition temperature T_c, for α- and γ-Ce using either a core or a band description for the $5p$ electrons. Here Θ_c is the high-temperature Debye temperature. We use the approximation $\langle \omega^2 \rangle^{1/2} = 0.69\Theta_c$.

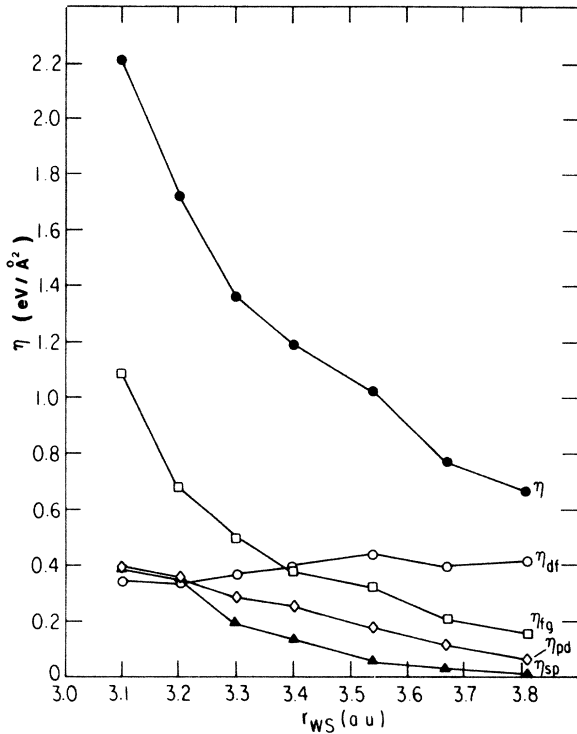|	$5p$ core α-Ce	$5p$ core γ-Ce	$5p$ band α-Ce	$5p$ band γ-Ce
$N(E_F)$ (Ry^{-1})	32.70	63.34	37.58	57.00
μ^*	0.13	0.13	0.13	0.13
Θ_c (K)	173	117	173	117
$\langle \omega^2 \rangle^{1/2}$ (K)	119	81	119	81
ω_{log} (K)	104	70	104	70
$M \langle \omega^2 \rangle$ (eV/Å^2)	3.550	1.645	3.550	1.645
η (eV/Å^2)	1.15	0.77	1.06	0.62
λ	0.32	0.47	0.30	0.37
T_c (K)	0.024	0.351	0.007	0.073

FIG. 5. Electron stiffness parameter η of the total and of each angular momentum channel as a function of Wigner-Seitz radius using LMTO atomic sphere potentials.

TABLE VI. Partial density of states N_l and total density of states $N(E_F)$ (in states/Ry atom), partial occupied charge Q_l, electron stiffness parameter $n_{l,l+1}$, η (eV/Å^2), electron-phonon coupling parameter λ, average phonon frequency $\langle \omega^2 \rangle^{1/2}$, and transition temperature T_c of α-Ce by treating one f electron as a core state. The same quantities for La are also provided for comparison.

	Ce ($r_{WS} = 3.54$)	La ($r_{WS} = 3.54$)
Q_s	0.49	0.45
Q_p	5.94	5.92
Q_d	2.10	2.20
Q_f	0.44	0.39
Q_g	0.03	0.03
N_s	1.04	1.09
N_p	0.82	0.83
N_d	13.43	12.64
N_f	7.53	4.75
N_g	0.24	0.26
$N(E_F)$	23.06	19.56
η_{sp}	0.14	0.20
η_{pd}	0.84	1.03
η_{df}	1.53	1.57
η_{fg}	0.13	0.11
η	2.64	2.91
$\langle \omega^2 \rangle^{1/2}$	119	86
λ	0.74	1.58
T_c (K)	3.26	8.13

those obtained from the FLAPW results. For example, $\eta = 0.67$ (γ-Ce) and $\eta = 1.02$ (α-Ce) in this (LMTO) case, compared with 0.62 and 1.06 in FLAPW. The results plotted in Fig. 5 show η increasing with pressure; η_{sp} and η_{pd} increase with pressure, while η_{df} is almost constant but somewhat decreasing. In fact, the steep increase of η orginates from the dominant behavior of η_{fg}, which implies that including g character ($l = 4$) is very significant in the investigation of the high-pressure superconducting properties of f-band metals, although the density and occupation of g states are very small, e.g., 0.26 states/Ry atom and only 0.03 electrons in the case of α-Ce. The occupation of g states increases slightly with increasing pressure and equals 0.06 at $r_{WS} = 3.1$. Note that η is only 0.6 for α-Ce without considering the g states. The large η_{fg} is attributed to the very small single scatterer density of states, $N_g^{(1)}(E_F)$, which determines the factor $v_g(N_g(E_F)/N_g^{(1)}(E_F))$ in Eq. (2). At $r_{WS} = 3.2$, v_g amounts to 4.69 compared with $v_s = 3.82$, $v_p = 0.45$, $v_d = 0.68$, and $v_f = 1.54$.

If we compare the calculated T_c (=0.02 K) with experiment for the lattice constant of α'-Ce, we find that it is smaller by two orders of magnitude than the experimental $T_c = 1.9$ K. As to the origin of this large discrepancy, it is not clear whether it is due to the underestimation of the electron stiffness parameter η in RMTA or due to the use of the α-Ce Debye temperature ($\Theta_D = 179$ K) which neglects phonon softening. Phonon softening, which is likely to accompany the structural transition to the α'-Ce phase, may affect the superconducting properties of α'-Ce. The use of a constant Coulomb parameter μ^*

(=0.13), also influences the transition-temperature results. The parameter μ^* is expected to decrease slightly with pressure. In fact, if we use the empirical formula of Bennemann and Garland,[34] μ^* is in the range of 0.22 (at $r_{WS} = 3.81$) and 0.18 (at $r_{WS} = 3.1$); these values are larger than the value we used (0.13) and thus, if used, will result in suppressed T_c values.

If one f electron in Ce is treated as a core state (as discussed in Sec. II), the corresponding electronic structure will be similar to that of La, even though screening of the extra nuclear charge by f-core electrons is not complete. As is shown in Table VI for $r_{WS} = 3.54$ a.u., there are only 0.05 more f-like conduction electrons occupied in Ce than in La and the resulting η's are very close, 2.6 for Ce and 2.9 for La, which are larger by a factor of 2 than those obtained previously. In this case, η_{pd} and η_{df} become dominant, whereas η_{fg} is substantially reduced for both materials. However, La has a much larger λ and T_c owing to the much smaller Debye temperature. This comparison suggests that the electronic stiffness parameter η in Ce can be large as in La in which case Ce becomes a possible candidate to be a $4f$ band superconductor—provided the f electrons are partially delocalized as above. The calculated T_c of α-Ce turns out to be much higher in this case, $T_c = 3.3$ K. Note however, that when we treat the f electrons of Ce as ordinary itinerant valence electrons, η is then much smaller than that of La.

VI. COULOMB CORRELATION AND LOCALIZATION OF f ELECTRONS

In contrast to the promotional model, we found that the f bands are broadened with pressure and that the number
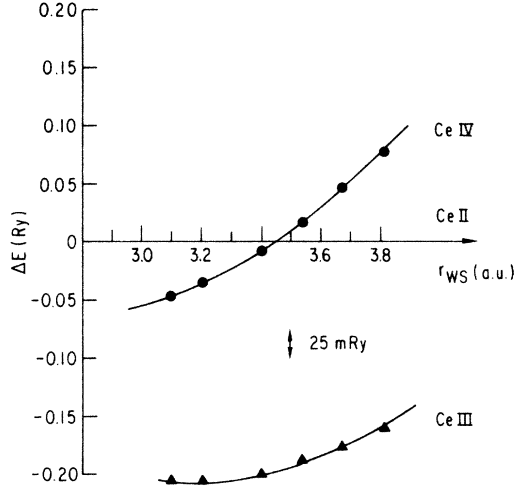
FIG. 6. LMTO total-energy differences of the trivalent (III) and tetravalent (IV) phases of Ce relative to that of the divalent (II) phase as a function of Wigner-Seitz radius. The $4f$ electrons are treated as core states.

of f electrons is constant. This result supports the localization and delocalization transition of the $4f$ electrons. In agreement with Johansson's[6] arguments based on empirical data, our calculations with the number of $4f$ electrons kept fixed in the core yield total-energy differences between trivalent and tetravalent configurations, which are overly large for α-Ce metal to be a promotional-type mixed-valent material. We plot the total energies of three valence configurations, i.e., divalent, trivalent, and tetravalent, as a function of Wigner-Seitz radius in Fig. 6 by treating the f electrons as core states. The trivalent configuration is lower in energy by about 2.4 eV than the tetravalent or divalent configurations over the range of lattice constants considered and the divalent configuration is more stable than the tetravalent at the lattice constant of α-Ce ($r_{WS}=3.54$ a.u.). The energy differences between the trivalent and tetravalent configurations amount to 3.2 eV for γ-Ce and 2.8 eV for α-Ce, which corresponds to the localized $4f$ excitation energies in the photoemission experiment.[19] From these total energies, we can obtain the intra-atomic Coulomb correlation interaction parameter U from the relation

$$U = E[f^0(5d,6s,6p)^4] + E[f^2(5d,6s,6p)^2]$$
$$- 2E[f^1(5d,6s,6p)^3] .$$

The resulting values of U are found to vary weakly between 5.0 and 5.6 eV over the volume range considered and to decrease with pressure.

Compared with the bandwidth of 0.78 eV for γ-Ce and 1.23 eV for α-Ce, the value of the Coulomb correlation U is much too large for the $4f$ band to delocalize, in the ordinary sense of the Hubbard model. Recently f-shell localization was discussed by Harrison.[35] He proposed a condition for the localization of f electrons, which is similar to the form obtained when an Anderson local moment

forms in a degenerate band. Qualitatively, Harrison's localization condition can be written as

$$p \equiv \frac{2U}{\pi} \frac{1}{W(4f)} \sin^2 \left[\frac{\pi n_f}{(2J+1)} \right] > 1 , \qquad (4)$$

where n_f is the number of occupied f electrons ($n_f = 1$ for Ce) and J is the total angular momentum of the f shell. When spin-orbit coupling is included, the ground state of Ce has $J = \frac{5}{2}$, which has a sixfold degeneracy. If we apply this relation [Eq. (4)] with values of the bandwidth (W) and Coulomb correlation U considered above ($W=1.23$ eV and $U=5.4$ eV for α-Ce and $W=0.78$ eV and $U=5.5$ eV for γ-Ce), we obtain $p=0.7$ for α-Ce and $p=1.1$ for γ-Ce. Hence this result indicates that γ-Ce is just inside the localized limit of f electrons, while α-Ce is in the region of delocalization. This result is consistent with the occurrence of f-band magnetism which was considered in Sec. IV.

In order to investigate the degree of f localization more quantitatively, we consider the spatial extent of the f orbital within the Wigner-Seitz atomic cell. By calculating the radial expectation value $\langle r \rangle$ of wave functions on the Fermi surface, we obtain the average distance of the valence electrons from the nucleus. The $\langle r \rangle$'s of $6s$, $5p$, $5d$, and $4f$ orbitals normalized by the Wigner-Seitz radius are displayed in Fig. 7 as a function of Wigner-Seitz radius. It is seen that $\langle r_f \rangle$ is much smaller than those of the other orbitals and thus shows clear evidence for the localized nature of the f electrons. The spatial extent of the $6s$ and $5d$ (conduction-band) orbitals is almost constant over the whole range of volumes shown, while that of the $5p$ and $4f$ orbitals increases monotonically with decreasing lattice constant. As discussed in Sec. II, the $5p$ electrons become greatly extended with pressure. However, $\langle r_f \rangle$ does not indicate any appreciable change between α- and γ-Ce (0.35 for γ-Ce and 0.37 for α-Ce). Note that if the f electrons in γ-Ce are treated as core states, $\langle r_f \rangle$ is reduced to 0.31. The dramatic change in the tail region of the $4f$ orbitals between α- and γ-Ce is seen when one calculates $\langle r^n \rangle$ values with higher n values.[8]
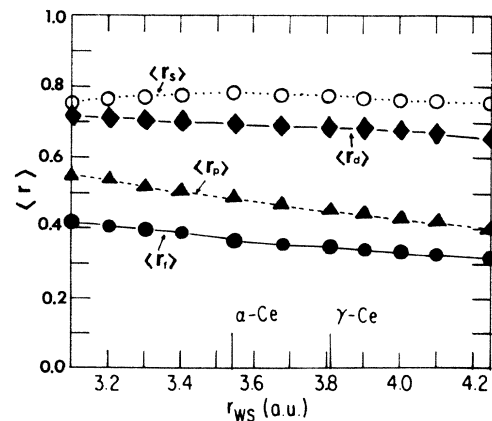

FIG. 7. Radial expectation values $\langle r \rangle$ of the wave functions of each orbital on the Fermi surface. Even value is normalized to the respective Wigner-Seitz atomic radius.

VII. DISCUSSION

Our calculation of the paramagnetic total energy does not show any dramatic features associated with the γ-α transition in Ce metal. One might expect that a spin-polarized calculation will reduce the f-bonding effect, as in the case of Am,[36] leading to some structure in the total energy curve. In fact, we found a magnetic instability close to the lattice constant of γ-Ce. The total-energy difference between the paramagnetic and ferromagnetic phases is overly small, however, to show clear evidence of a first-order phase transition; only a small change of curvature can be seen in Fig. 3. The transition pressure which can be obtained using a Maxwell construction in the total energy versus volume plot amounts to -120 kbar, which is of the same order of magnitude as Glötzel[7] obtained from his pressure calculation. Compared with the experimental transition pressure $(P = -10$ kbar) at zero temperature, which is the extrapolated value from the γ-α phase line, our estimated transition pressure is larger by one order of magnitude. This large discrepancy implies that a spin-polarized calculation for Ce does not adequately describe the localization of the $4f$ electrons, unlike the case of Am which has about six $5f$ electrons in an almost half-filled band. Our calculation[29] for bcc Eu, which has almost seven fully polarized $4f$ electrons, shows a similar behavior; a spin-polarized calculation substantially improves the error in the lattice constant, but is still 5% off from experiment. When we consider the $4f$ electrons in Eu as core states, we find the equilibrium Wigner-Seitz radius to be 4.33 a.u., which is close to the experimental value $(r_{\text{WS}} = 4.29)$. This example indicates that the $4f$ electrons in the heavy rare-earth metals are very localized, so that the bonding effect of the $4f$ electrons can be neglected. In Ce, however, the degree of hybridization of the $4f$ electrons is smaller than that predicted by LDA, but is not negligible (in fact, Ce metal under high pressure acts much like a $4f$-band metal), which makes a localization description difficult.

The actual volume collapse during the γ-α transition indicates that the electron-phonon interaction is an important factor. Hence, it is expected that some anomaly will be seen in the phonon spectra which is associated with a possible softening in the transition arising from the electronic contribution, as is discussed for La by Pickett et al.[37] To our knowledge, no phonon spectra of α-Ce are available to date due to the difficulties of sample preparation. Once available, the comparison of phonon spectra in the various phases of Ce metal will yield crucial insights into the nature of the phase transition as well as superconducting properties.

*Present address: Department of Physics, Oregon State University, Corvallis, OR 97331-6507.

[1]D. C. Koskenmaki and K. A. Gschneidner, in *Handbook on the Physics and Chemistry on Rare Earths,* edited by K. A. Gschneidner and L. R. Eyring (North-Holland, Amsterdam, 1978), Vol. I, p. 337.

[2]E. Ponyatovskii, Dokl. Akad. Nauk SSSR **120,** 1021 (1959) [Sov. Phys.—Dokl. **3,** 498 (1959)]; A. Jayaraman, Phys. Rev. **137,** A179 (1965).

[3]W. H. Zachariasen (unpublished) quoted in A. W. Lawson and T. Y. Tong, Phys. Rev. **76,** 301 (1949); L. Pauling, J. Am. Chem. Soc. **69,** 542 (1947); B. Coqblin and A. Blandin, Adv. Phys. **17,** 281 (1968); R. Ramirez and L. M. Falicov, Phys. Rev. B **3,** 1225 (1971).

[4]See, for a review, J. M. Lawrence, P. S. Riseborough, and R. D. Parks, Rep. Prog. Phys. **44,** 1 (1981).

[5]D. R. Gustafson, J. D. McNutt, and L. O. Roelling, Phys. Rev. **183,** 435 (1969).

[6]B. Johansson, Philos. Mag. **30,** 469 (1974).

[7]D. Glötzel, J. Phys. F **8,** L163 (1978).

[8]W. E. Pickett, A. J. Freeman, and D. D. Koelling, Phys. Rev. B **23,** 1266 (1981).

[9]R. Podloucky and D. Glötzel, Phys. Rev. B **27,** 3390 (1983).

[10]R. D. Parks, N. Martensson, and B. Reihl, in *Valence Instabilities,* edited by P. Wachter and H. Boppart (North-Holland, Amsterdam, 1982), p. 239; D. M. Wielczka, C. G. Olson, and D. W. Lynch, Phys. Rev. B **28,** 3028 (1984).

[11]J. W. Allen and R. M. Martin, Phys. Rev. Lett. **49,** 1106 (1982); see also R. M. Martin, *ibid.* **48,** 362 (1982).

[12]M. Lavagna, C. Lacroix, and M. Cyrot, J. Phys. F **13,** 1007 (1983).

[13]S. Doniach, Physica B **91,** 231 (1977).

[14]O. Gunnarsson and K. Schönhammer, Phys. Rev. B **28,** 4315 (1983).

[15]A. Fujimori, Phys. Rev. B **28,** 4489 (1983).

[16]S. Hüfner and P. Steiner, Z. Phys. B **46,** 37 (1982).

[17]S. H. Liu and K.-M. Ho, Phys. Rev. B **28,** 4220 (1983).

[18]P. Hohenberg and W. Kohn, Phys. Rev. **136,** B864 (1964); W. Kohn and L. J. Sham, *ibid.* **140,** A1133 (1965).

[19]M. R. Norman, D. D. Koelling, A. J. Freeman, H. J. F. Jansen, B. I. Min, T. Oguchi, and Ling Ye, Phys. Rev. Lett. **53,** 1673 (1984); B. I. Min, H. J. F. Jansen, T. Oguchi, and A. J. Freeman, Phys. Rev. B **33,** 8005 (1986).

[20]E. A. Kmetko and H. H. Hill, J. Phys. F **6,** 1025 (1976).

[21]O. K. Andersen, Phys. Rev. B **12,** 3060 (1975).

[22]D. D. Koelling and G. D. Arbman, J. Phys. F **5,** 2041 (1975).

[23]C. Probst and J. Wittig, in *Handbook on the Physics and Chemistry of Rare Earths,* edited by K. A. Gschneidner and L. R. Eyring (North-Holland, Amsterdam, 1978), Vol. I, p. 749.

[24]J. Wittig, in *Festkörperprobleme,* edited by. H. J. Queisser (Vieweg, Braunschweig, 1973), Vol. XIII, p. 375.

[25]H. J. F. Jansen and A. J. Freeman, Phys. Rev. B **30,** 561 (1984).

[26]D. D. Koelling and B. N. Harmon, J. Phys. C **10,** 3107 (1977).

[27]V. von Barth and L. Hedin, J. Phys. C **5,** 1629 (1972).

[28]L. Hedin and B. I. Lundqvist, J. Phys. C **4,** 2064 (1971).

[29]B. I. Min, H. J. F. Jansen, T. Oguchi, and A. J. Freeman, J.

Magn. Magn. Mater. (to be published).

[30]T. J. Watson-Yang, B. N. Harmon, and A. J. Freeman, J. Magn. Magn. Mater. **2**, 334 (1976); J. F. Janak, Phys. Rev. B **16**, 255 (1977).

[31]G. D. Gaspari and B. L. Gyorffy, Phys. Rev. Lett. **28**, 801 (1972).

[32]W. L. McMillan, Phys. Rev. **167**, 331 (1968).

[33]P. B. Allen and R. C. Dynes, Phys. Rev. B **12**, 905 (1975).

[34]K. H. Bennemann and J. W. Garland, in *Superconductivity in d- and f-Band Metals (Rochester)*, Proceedings of the Conference, on Superconductivity in d- and f-Band Metals, AIP Conf. Proc. No. 4, edited by D. H. Douglass (AIP, New York, 1972) p. 103.

[35]W. A. Harrison, Phys. Rev. B **29**, 2917 (1984).

[36]H. L. Skriver, O. K. Andersen, and B. Johansson, Phys. Rev. Lett. **44**, 1230 (1980).

[37]W. E. Pickett, A. J. Freeman, and D. D Koelling, Phys. Rev. B **22**, 2695 (1980).